Incorporating Muscle Activation Dynamics into the Global Human Body Model

Lacie Feller, Christian Kleinbach, Jörg Fehr, Syn Schmitt

Abstract Over 20 million injuries result every year from motor vehicle collisions, with injuries to the neck being among the most prevalent. Muscle activity has been shown to affect head and neck kinematics significantly, especially in low-speed collisions. The present study develops the framework to introduce strain-dependent muscle activation into a widely available computational human body model (HBM) and study the effects on head and neck kinematics. A single MAT_156 beam element from the Global Human Body Models Consortium (GHBMC) model in combination with a user-defined subroutine to compute activation levels is used to model active force contributions of a full muscle. The model is validated against contraction velocities of experimental porcine tests, which are loaded with masses of 100−800 grams. CORA ratings between simulation and experimental results range from 0.538 to 0.810. Finally, we incorporate this strain-dependent muscle activation scheme into the neck of the GHBMC for a low-loading condition through a head fall test. Though the neck is too stiff when compared with volunteer data, simple modifications may be made to the model which results in closer agreement with experimental findings.

Keywords Biofidelity, Finite Element model, GHBMC, Human Body Modelling, Muscle activation

I. INTRODUCTION

Motor vehicle collisions (MVC) cause over one million deaths and 20 million injuries every year [1]. In Europe alone, this results in annual costs of over €160 billion [2]. Neck strain and sprains are the most commonly reported injuries resulting from MVC, comprising 27.8% of all motor vehicle injuries in U.S. emergency rooms [3]. Each cervical spine injury claim costs Europe an average of €9,000 [4]. These injuries are not only frequent, but often chronic. Half of all whiplash patients still report symptoms one year after the initial hospital visit [5]. To reduce the incidence of injury, it is necessary to model the occupant response as accurately as possible. The development of computational human body models allows vehicle safety design to be optimised for humans rather than anthropometric test devices.

Previous studies suggest that incorporating muscle activity into computational models at lower impact speeds is necessary for a biofidelic response in the neck [6], while the effects of muscle activity are more disputed at higher severity impacts. This has been attributed to both the relatively long latency period of muscle contraction when compared with the duration of impact [7−9], as well as the high forces imparted on the occupant that cannot be overcome by forces produced by muscle contraction [8]. Muscle activation has been included in many computational HBMs. Some use static activation levels optimised for a specific position [10], while others use predefined time-activation curves [11]. Within the context of cervical muscle activation, many studies use the acceleration of the T1 vertebra as an indicator for the onset of muscle activity [6,11]. More recent approaches avoid solving the inverse dynamics problem and use feedback control to simulate posture maintenance [12] or changes in posture [13−14] but generally rely on macroscopic kinematic parameters such as neck or elbow angles as inputs for the controller. While these approaches may be appropriate for voluntary occupant responses, they neglect the physiology that causes a monosynaptic stretch reflex that regulates the length of skeletal muscle. Muscle spindles are responsible for sensing changes in length and conveying this information to the nervous system. This in-vivo stretch reflex is activated by lengthening of the muscle spindle which signals the nervous system to increase alpha motor neuron activity, resulting in muscle contraction to resist lengthening.

Dr J. Fehr (email: joerg.fehr@itm.uni-stuttgart.de; tel: +49 711-685-66392) is a professor, L. Feller is a visiting Fulbright student, and C. Kleinbach is a research associate and doctoral student at the Institute of Engineering and Computational Mechanics at the University of Stuttgart. Dr S. Schmitt is a professor at the Institute of Sport and Exercise Science at the University of Stuttgart. All contributors are members of the SimTech Cluster of Excellence at the University of Stuttgart.

Whereas many studies regarding muscle activation and muscle response at lower speeds are performed with multibody models [15−16], finite element (FE) methods allow users to build more intricate models that describe the human body in great anatomical detail. In addition, the automotive industry has the complete surrounding environment for the HBM, e.g. car, interior, seat, etc. available as FE models. This allows an easy setup of correct boundary conditions and multiple simulation scenarios. The Global Human Body Model Consortium-owned GHBMC model M50-0 v. 4.3 [17−18] is an FE model developed for use with LS-DYNA and has been validated at the individual vertebrae and full cervical spine level [17,19−31]. The GHBMC includes passive 3D muscle representations, as well as 1D beam elements for active muscle contraction. Fig. 1 displays the beam elements which comprise the 1D neck musculature of the GHBMC. These beam elements are modelled using MAT_156, routed along 91 unique muscle paths in the neck, and include force-length and force-velocity effects. MAT_156 is an LS-DYNA material model based on a Hill-type muscle model with a parallel damper. The standard approach is to define activation level over time within the material definition a priori to the simulation. Other approaches use controllers to calculate activation levels at a high-level hierarchy based on macroscopic kinematic parameters. These activation levels have to be calculated for every forward simulation, e.g. with optimisation procedures. The main contribution of this work is the demonstration of a closed-loop online calculation of the activation level at a lower level hierarchy replicating reflexive muscle behaviour including muscle activation dynamics.

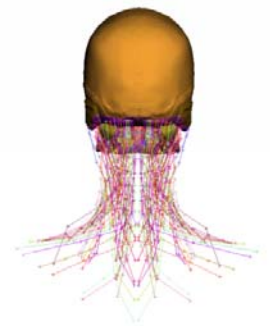

Fig. 1. 1D muscle beam element geometry included in the neck region of the GHBMC.

Reflexive muscle behaviour calculated by closed-loop control allows the activation level to be controlled by neural stimulation and eliminates the need to calculate muscle activation schemes beforehand. In this paper, activation levels are calculated based on the muscle strain in an effort to model the response of the muscle spindles and all calculations to determine activation level are performed during runtime. In LS-DYNA version R8.0 a combination of *DEFINE_CURVE_FUNCTION and PIDCTL exist to implement some rudimentary control so that activation dynamics can be determined dynamically. However, the implementation of an activation scheme based on *DEFINE_CURVE_FUNCTION and PIDCTL is very cumbersome, and it is not possible to include additional degrees of freedom. Therefore, the control law is implemented as a user-defined function. The approach has the advantage of being readily incorporated into different body regions, as it is not dependent on a fixed posture in a specified body region and can be easily adapted by future users to incorporate more complex activation schemes.

First, our activation method is validated in a single muscle model using the MAT_156 formulation in combination with the user-defined control function against experimental porcine muscle contraction tests. Second, the validated results are transferred to the GHBMC model. In a first study, the GHBMC model is then run passively in a head fall test to ensure that the stiffness of the neck is appropriate for low loading conditions. Finally, we test the suitability of our muscle activation scheme when inserted into a modified neck of the GHBMC under a low severity loading condition.

II. METHODS

In this section, we describe a general approach to improve the modelling of muscle activation by using a user-defined function.

uctrl1 Subroutine for Implementing Activation Dynamics

The standard approach for activation of a MAT_156 muscle element is to use a predefined curve function. The ”uctrl1” subroutine can instead be used to calculate activation levels during runtime and return these

values for use in conjunction with the passive properties of the MAT_156 material model, as outlined in Fig. 2. The load curves in the material data card must be replaced by an empty dummy curve specifying only the curve number. However, using a subroutine allows activation level to be computed at each time step based on the current state of the simulation. In order to implement reflexive muscle activity into the GHBMC, a Fortran subroutine for LS-DYNA (version R7.1.2, LSTC, Livermore, USA) is developed. Within this subroutine, the 1D engineering strain $\varepsilon_{\mathrm{Muscle}}$ of every beam element in a 1D muscle is calculated. When a specified strain threshold is surpassed, a delay is implemented before beginning the activation scheme. Afterwards, the user-defined "uctrl1" function will return a value for the appropriate curve number, representing the activation level a, at each time step. Therefore, the activation level used in the MAT_156 muscle element is based on the activation level calculated within uctrl1. The activation level is then translated by the MAT_156 material model to a force exerted by the muscle.

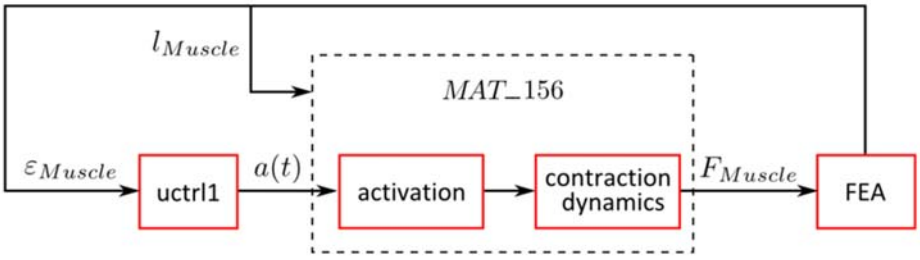

Fig. 2. Implementation of the uctrl1 subroutine to activate muscles within LS-DYNA.

Activation dynamics, modelled by a first order differential equation [32], is used to compute muscle activation level at every time step after the strain threshold and initial time delay have been surpassed, or the muscle returns to its initial length:

$$\frac{da}{dt} = \frac{u - a}{\tau(a,u)}$$

$$\tau(a,u) = \begin{cases} t_{\mathrm{act}}(0.5 + 1.5a) & u > a \\ \dfrac{t_{\mathrm{deact}}}{0.5 + 1.5a} & u \leq a \end{cases}$$

where, t is time, a is current activation level, u is neural excitation, τ is a variable time coefficient, and $t_{\mathrm{act}} = 10$ ms and $t_{\mathrm{deact}} = 40$ ms are known activation and deactivation constants [33–34].

Unfortunately, not all constants needed to determine activation dynamics are well-defined. No information was found in literature for the amount of lengthening required to induce muscle activity, while values for latency have been reported in the range of 21.3–27.7 ms [35]. While a 34 ms neural delay used in [13], our model simulates a reflex arc which eliminates the processing necessary for conscious resistive feedback and thus the response time should be quicker. In an earlier study on muscle activity in the cervical spine, a delay of 25 ms is chosen [6]. In order to determine an appropriate strain threshold for initial implementation purposes, the muscles were simulated using LS-OPT (version 5.2, LSTC, Livermore, USA) with strain thresholds ranging from 1 to 10%, with 5% strain resulting in a strong correlation with experimental data. An initial parameter optimisation was performed with single muscle tests and CORA software described below, from which a delay of 24.5 ms and 5% strain threshold were chosen for initial simulations.

The intention of this work is the development of a rather general computation method to allow incorporation of advanced activation and control schemes in a standard FE program. The approach uses user-defined functions to implement the control scheme. Therefore, the approach allows very flexible extensions, no simulator coupling, e.g. to Matlab, is necessary, and the approach can be easily transferred to every LS-Dyna HBM using Mat_156 muscles, e.g. THUMS [36].

Single Muscle Test

To validate these methods, experimental studies that determined the force vs. velocity characteristics of porcine muscles by loading them with varying masses as outlined in [37] are replicated on the level of a single

muscle. A MAT_156 beam element with a length of 59.7 mm and a cross-sectional area of 25 mm^2 is used to represent a muscle. The default force-velocity and force-length properties of the GHBMC are used, and the activation level is determined by the described subroutine. In the simulation, one end of the muscle is constrained in all translational and rotational degrees of freedom (DoF), while the node at the opposite end of the muscle is loaded with masses ranging from 100 to 800 g.

A comparison between contraction velocity of the MAT_156 beam elements and experimental data, when subjected to a 100 g mass, can be seen in Fig. 3. The simulated muscle initially lengthens due to the force of the weight. After the strain threshold of 5% is surpassed at 68.6 ms, the muscle continues to lengthen until the delay time is surpassed and the force produced by muscle contraction overcomes the force exerted by the weight. The activation level continues to increase until the muscle returns to its initial length, at which point the neural excitation is changed from 1 to 0, and the activation level gradually decreases, resulting in a decreasing contraction velocity. As only shortening velocities are available from the experimental data, the initial lengthening velocities are removed from simulation data, see Fig. 3. The processed experimental data is then used to evaluate the correlation. A sensitivity analysis of the correlation is also performed. The values for neural delay (18.1−30.9 ms) are chosen such that they are within two standard deviations of the average values found in [35]. Variations in strain threshold were initially set from 1−10% in order to limit the muscle lengthening to a range in which no damage would occur. Little information exists regarding the exact measure of muscle strain needed to induce reflexive shortening, but tearing of stimulated muscles occurs at approximately a 25% length increase [38]. Changes in the muscles were seen after repeated eccentric contractions were performed under loading conditions with strains as low as 12.5% [39].

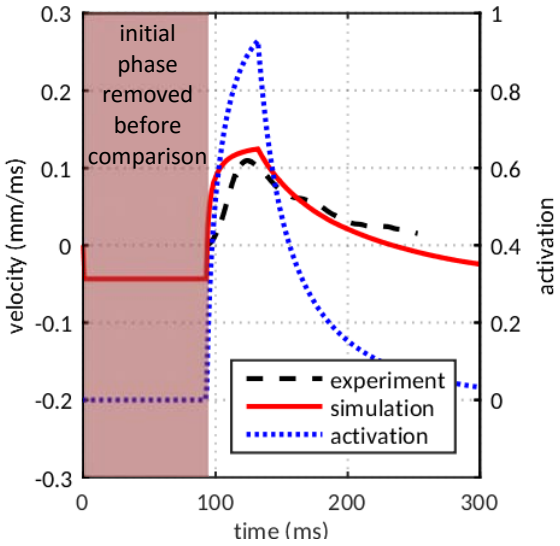

Fig. 3. Comparison of muscle contraction velocity between experiment and simulation (including lengthening velocities) against 100 g mass with activation profile of the simulated muscle included.

The comparison between simulated muscle velocity and experimental measurements is performed in the time domain with CORA [40]. The software CORA (CORelation and Analysis) provides an effective analysis of time signals when used to compare experimental and simulation results in the vehicle safety context. The rating consists of corridor and cross-correlation components. The latter can be further broken down into curve phase, size, and shape criteria, as described in Fig. 4. The weighting factors used were left at the default values set by CORA, which can be found in Table I.

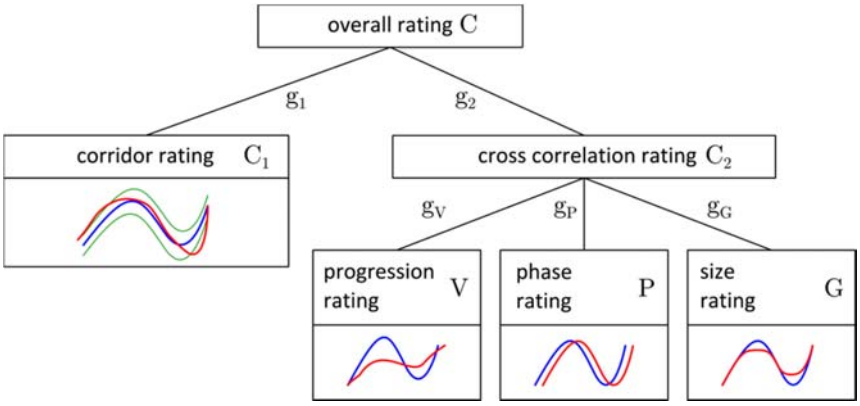

Fig. 4. Calculation of CORA rating between simulation and experimental curves.

TABLE I
CORA FACTORS USED IN THIS STUDY

g_1	50%
g_2	50%
g_V	50%
g_P	25%
g_G	25%

Head Fall Test

Once we know our activation method produces reasonable results, the same workflow is applied to the human neck where more than 900 muscle segments must be controlled. The neck of the GHBMC is modelled with 3D passive muscles and uses 1D MAT_156 beam elements to model the active muscles. 3D muscles were not changed from the original GHBMC model. To implement active muscle function, each muscle beam element in the neck of the GHBMC is assigned its own material and part ID, and the beam elements are activated individually by the same subroutine described above. The parameters from the initial optimisation, a 5% activation threshold and 24.5 ms delay, are implemented in the GHBMC neck muscle elements. In order to minimize calculation time, the model is reduced to the head, neck, and torso. For model validation at low accelerations, the GHBMC is used to replicate a volunteer "head fall" test, as shown in Fig. 5. For the experiment, a group of seven male subjects were asked to lie on a table, the head was positioned over a trap door, and subjects were asked to relax their muscles. The trap door was then released, and the head moved according to external gravitation. In the simulation, gravitational acceleration is applied to the body while movement of thorax and inferior nodes are constrained in all translational and rotational DoF, resulting in downward translation and rotation of the head. The test is run first without active muscle contributions to obtain a baseline for head motion. The vertical displacement of the head centre of gravity (COG) is compared with experimental results. As the model is quite sensitive to the vertebral constraints chosen, and the exact movement of the vertebrae in volunteer subjects is not known, simulations with constraints beginning at different vertebrae are performed.

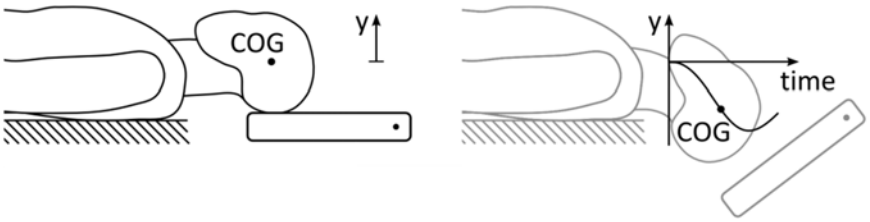

Fig. 5. Experimental head fall tests are replicated using the GHBMC, and the vertical displacement of the COG is evaluated.

III. RESULTS

Single Muscle Test

A comparison between contraction velocity of the experimental and simulated muscle, when loaded with masses of 100 to 800 g, are shown in Fig. 6. For all load cases, muscle shortening velocity decreases with increased loading, and peak contraction velocity is reached within 70 ms of the onset of muscle shortening. CORA analysis with an overall correlation value of 0.639 was performed on the velocity curves. The technical report ISO/TR 9790 defines a qualitative sliding scale for CORA ratings, ranging from excellent to unacceptable.

Muscles loaded with 200 to 600 g masses produced a CORA rating of "fair", whereas stronger correlations rated as "good" were found at the ends of the loading spectrum tested (100 and 800 g), as outlined in Table II. A sensitivity analysis of the chosen values can be found for strain threshold in Table III and for neural delay in Table IV. For the purpose of the sensitivity analysis, all variations in strain threshold were performed with a 24.5 ms delay, and all variations in time delay were performed with a constant 5% strain threshold. The results indicate that within the specified ranges, variations in the strain threshold have a greater effect on the correlation results than variations in time delay.

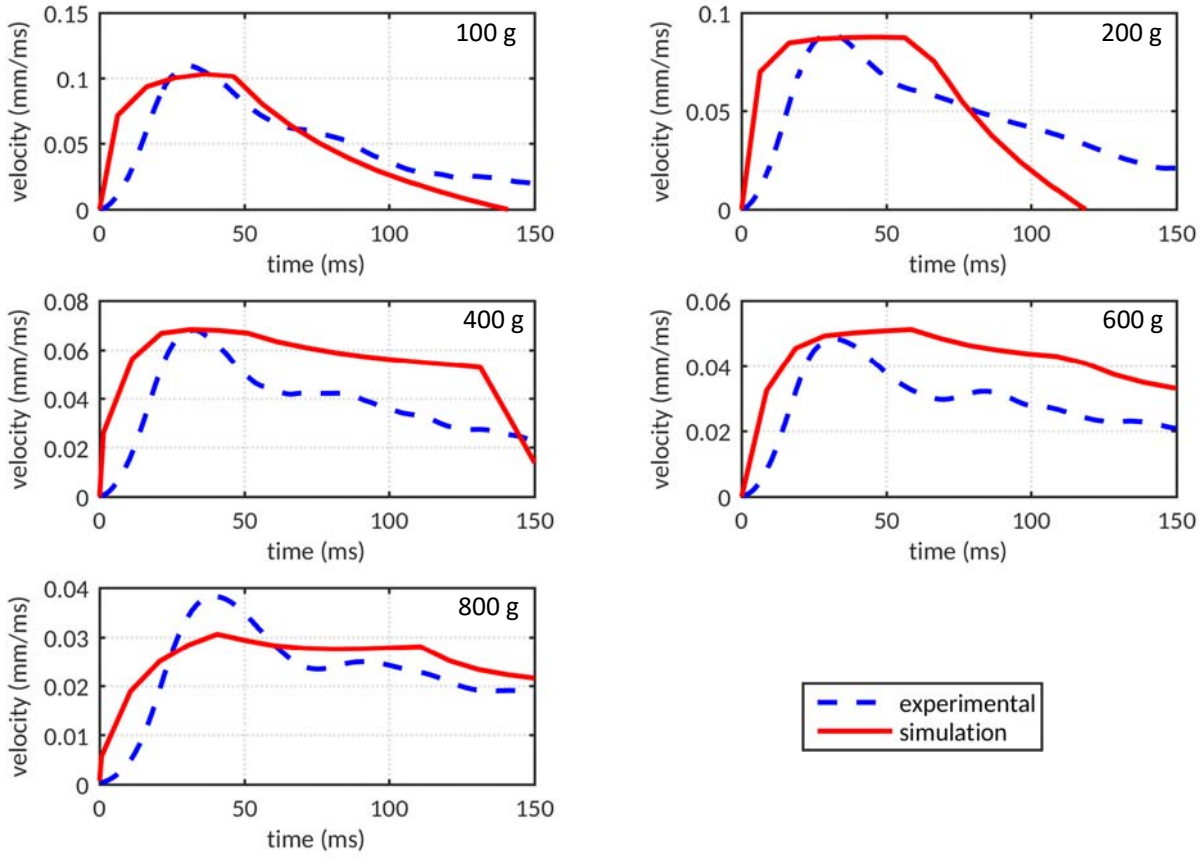

Fig. 6. A comparison of muscle contraction velocity when loaded with 100, 200, 400, 600, and 800 g masses.

TABLE II
CORRELATION DATA FOR MUSCLE CONTRACTION VELOCITY

Mass (g)	CORA Rating	
100	0.752	Good
200	0.548	Fair
400	0.538	Fair
600	0.538	Fair
800	0.810	Good
Overall	**0.639**	**Fair**

TABLE III
SENSITIVITY OF CORRELATION DATA TO STRAIN THRESHOLD

Strain Threshold (%)	CORA Rating
1	0.578
2	0.587
3	0.619
4	0.630
5	0.639
6	0.662
7	0.659
8	0.647
9	0.651
10	0.639

TABLE IV
SENSITIVITY OF CORRELATION DATA TO TIME DELAY

Neuromuscular Delay (ms)	CORA Rating
18.1	0.653
21.3	0.637
24.5	0.639
27.7	0.663
30.9	0.656

Head Fall Test

The average male experimental response during the head fall tests can be compared with responses seen using the GHBMC in Fig. 6. Initially, the vertebrae of the GHBMC were constrained from T1 downward. With these constraints the head COG displacement of the passive GHBMC is lower than that of the middle 50th percentile of experimental subjects. While male subjects experience an average maximum displacement of 79.7 mm that occurs 191 ms after head release before the force produced by the muscles can overcome that of gravity, the GHBMC without active muscle contributions has 31.3 mm of displacement occurring over a time period of 162.5 ms. Subsequently the constrains were changed to constrain all movement from T3 downward, allowing translational and rotational movement of T1 and T2. This is likely a more realistic representation of the motion occurring and results in a further displacement of the head to 45.3 mm. The model with vertebral constraints beginning at T3 is then used for the remaining simulations, as further reduction of the constraints was deemed unrealistic in the experimental setup.

To determine which components are absorbing additional energy and increasing the stiffness of the model, the internal energy of the tissues found in the neck are plotted in Fig. 7. As would be expected by their relatively large volume in the neck and the deformation seen in simulation, the 3D muscles absorb a large amount of energy. The 1D ligamentous structure elements absorb relatively little energy in comparison. Unexpectedly, the parts comprising the skin absorb more energy than any of the other components studied. In order to determine the contributions to neck stiffness added by the skin, all three layers were removed from the model. When the skin is removed, the maximum displacement of the head COG is 91.5 mm. Simulation results of the modified neck now fall within one standard deviation (51.6−107.8 mm) of the male experimental responses, and the passive head and neck model falls farther than the average volunteer with active muscle responses.

When muscle activation dynamics are added to the model without skin, maximum displacement is reduced and occurs earlier. The first muscles from the flexor group begin to activate at 69.4 ms. As more muscle elements pass the strain threshold and are recruited, the neck flexes back upward after reaching its maximal displacement of 65.7 mm at 186 ms. The recruitment of muscles within the flexor and extensor groups is shown in Fig. 8 and 9, with the contributions of the flexors outweighing that of the extensors. Of the 250 flexor beam elements, 28 were activated during the simulation. Of the 666 extensor elements, only six were activated.

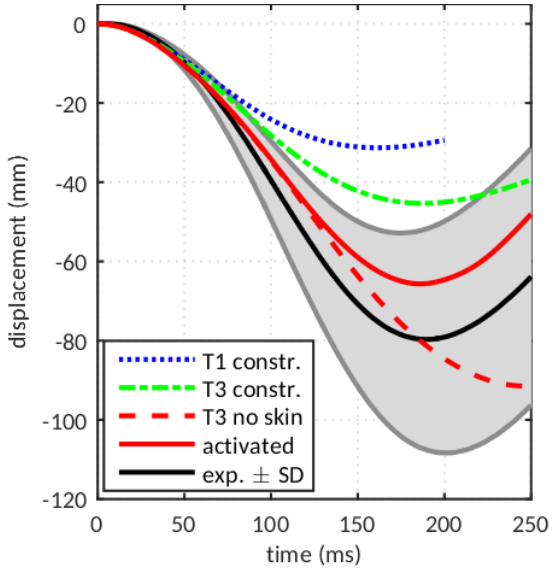

Fig. 6. Displacement resulting from head fall test when modifications to the GHBMC are made to alter neck stiffness.

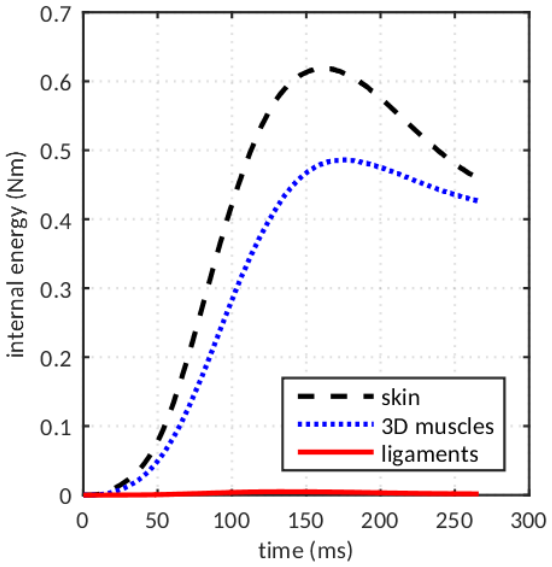

Fig. 7. Internal energy in different parts of the neck during head fall test with vertebral constraints beginning at T1.

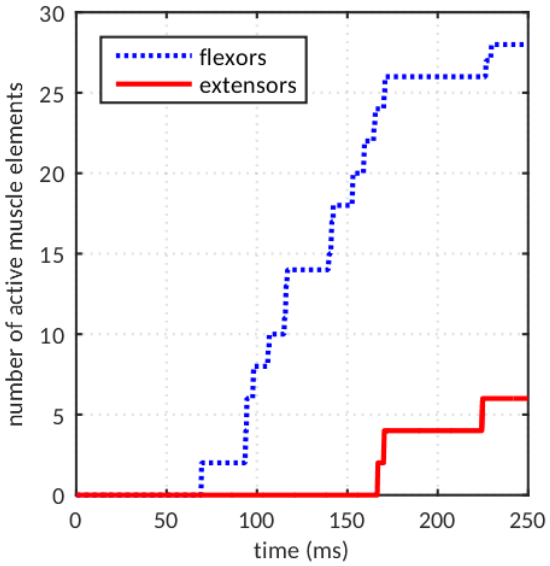

Fig. 8. Comparison of the number of flexors versus extensor beam elements activated during the simulated head fall tests.

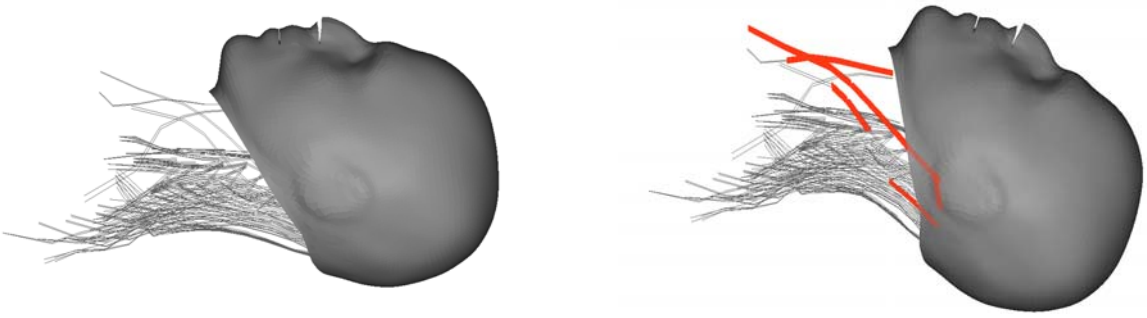

Fig. 9. Activated muscle elements during a head fall test are highlighted in red, while inactive elements remain grey. Shown on the right is the end state of the model (time = 250 ms), which can be compared to the initial state on the left.

IV. DISCUSSION

Validation of the activation dynamics subroutine and resulting muscle model was performed by replicating porcine contraction tests. The general agreement between experimental and simulation results in both contraction velocity magnitude and timing indicate that MAT_156 is a sufficiently complex model for modelling active and passive properties on the full muscle level. Peak shortening velocity in simulation occurs between 40 and 70 ms, with an average time of 52 ms after muscle activity onset. If peak velocity is assumed to correspond to peak activity, the data is well aligned with literature that has found a 55 ms delay between the onset of muscle activity and peak activation level [6].

Greater impact velocities have been shown to result in a decreased time to onset of muscle activity in occupants. When volunteer subjects in rear-speed collisions were subjected to changes in velocities of 4 km/h and 8 km/h, muscle activation occurred earlier in subjects at the higher impact speed [41]. As the strain threshold is reached more quickly in our model with higher loading scenarios, the muscle activation time decreases with increased loading. Strain rate dependencies have not yet been fully included in the model, despite their potentially large effects. These effects will be included in the neural excitation factor. Neural excitation has been shown to vary based on the load, from 0.54 to 0.99 within the loading range of interest, with larger loads resulting in higher excitation values [37].

Though the initial values for neural delay and strain were determined through a parameter study, a sensitivity analysis reveals that more optimal values may still exist. While the influence of a small change in time delay does not largely affect the correlation results, the model is more sensitive to the values chosen for the strain threshold. Though the initial subroutine begins with what the authors believe to be reasonable values for strain activation threshold and muscle latency, further work must be done to determine the optimal values for an average male subject, optimising based on a full human model rather than a single muscle test. Due to the 74 hour run time of the simulation across 20 CPUs, an MPP compatible version of the subroutine should be implemented before further parameter modification is tested.

Muscle activity can significantly affect the movement of the head and neck in low-speed collisions [42]. If the GHBMC is to be used in these scenarios, it is important to begin with a passive neck stiffness that resembles a relaxed occupant. Though the GHBMC neck has been validated in frontal, rear and side impact, validation scenarios found in [28−31] represent more severe impacts than is suitable for studying muscle activity in the head fall test. While neck displacement timing of the model agrees very well with experimental results, the magnitude of the displacement, though within one standard deviation of experimental data, is still below the one of an average male volunteer. Reducing the stiffness of the neck that results from the skin offers one possible mechanism to improve kinematics, but the model may still need further stiffness reduction.

The activation of flexor muscles in response to head extension in Fig. 8 and 9 indicate that overall, the correct muscles are activated by the subroutine. The results of the sensitivity analysis and the activation of elements belonging to the extensor group indicate that improvements can still be made to the model. The first of which may be increasing the strain threshold required to begin the muscle activation process. This would allow the head to fall farther and fewer extensors would be likely to reach the strain threshold. There also exists the question of whether to activate single beam elements or the entire muscle. In the initial implementation, beam elements are activated individually which is based on the physiology of a muscle spindle. They are embedded in muscle fibres, which are bundled into fascicles with an average length of 1.5-18.2 cm in the neck [43]. This is close to the length of a beam element in the GHBMC model, which fall in the range of 0.49-7.66 cm. This approach justifies the use of muscle spindle delay and strain threshold parameters for the activation scheme. A more physiologically representative approach to be tested in future iterations may be to continue to analyse the strain in individual beam elements, but activate the entire muscle when the strain threshold is surpassed. This would allow for a more straightforward comparison of the cross-sectional area of the activated muscles across different muscle groups. Controlling the whole muscle would also be necessary in order include occupant bracing and other voluntary movement in future iterations.

The present work is most relevant when considered in the context of a relaxed volunteer, as no pre-impact bracing response or other voluntary responses are included, but protective muscle reflex activity is considered. The control approach used will also allow for the inclusion of more advanced activation dynamic models, such as the model proposed by Hatze [44], or an intentional occupant manoeuvre. This approach also allows for the development of a hierarchical approach where the neural stimulation either stems from a stretch mediated

response or from an intentional movement initiated in the brain. The conscious movement could be calculated by the highest hierarchy of the control loop and could be composed of a feedforward control in combination with inverse dynamics similar to the control used for robotic manipulators.

V. CONCLUSIONS

In this study, strain-dependent muscle activation dynamics were developed for use in a standard muscle material model used in FE-HBMs through a subroutine in LS-DYNA. When the activation dynamics were tested under a set of loading conditions, timing and magnitude of shortening velocity of the muscles agreed well with literature and experimental results. Initial parameters used to calculate activation and excitation levels resulted in CORA ratings of "good" and "fair" when compared to experimental data, though correlation can be improved by further study of the critical parameters. To determine its suitability for low-impact loading scenarios, the GHBMC was subjected to a head fall test in both active and passive modes. After modifications to reduce neck stiffness, magnitude and timing of the displacement are in reasonable agreement with experimental results. These results suggest feasibility of the activation method to describe reflexive muscle activation dynamics within the FE-HBM for use in predicting head and neck kinematics in low-severity impact scenarios.

VI. ACKNOWLEDGEMENTS

The authors would like to thank the German-American Fulbright Commission and the German Research Foundation (DFG) for financial support of the project within the Cluster of Excellence in Simulation Technology (EXC 310/1) at the University of Stuttgart. In addition, the authors would like to thank the reviewers for their comments to improve the manuscript.

VII. REFERENCES

[1] Jarawan, E., Mohan, D., *et al.* 2004 World report on road traffic injury prevention.

[2] Commision of the European Communities. (2001) White Paper European Transport Policy for 2010: time to decide.

[3] Quinlan, K.P., Annest, J.L., Myers, B., Ryan, G., and Hill, H. (2004) Neck strains and sprains among motor vehicle occupants—United States, 2000. *Accident Analysis & Prevention*. **36**(1): pp. 21-27.

[4] Chappuis, G. and Soltermann, B. (2008) Number and cost of claims linked to minor cervical trauma in Europe: results from the comparative study by CEA, AREDOC and CEREDOC. *European Spine Journal*, 17(10): pp. 1350-1357

[5] Carroll, L.J., Holm, L.W., *et al*. (2009) Course and prognostic factors for neck pain in whiplash-associated disorders (WAD): results of the bone and joint decade 2000–2010 task force on neck pain and its associated disorders. *Journal of manipulative and physiological therapeutics*, **32**(2): pp. S97-S107.

[6] Van der Horst, M.J., Thunnissen, J., Happee, R., Van Haaster, R., and Wismans, J. The influence of muscle activity on head-neck response during impact. *SAE Conference Proceedings*, 1997.

[7] De Jager, M., Sauren, A., Thunnissen, J., and Wismans, J. Global and a detailed mathematical model for head-neck dynamics. *Proceedings of the Stapp Car Crash Conference*, 1996.

[8] Khodaei, H., Mostofizadeh, S., Brolin, K., Johansson, H., and Östh, J. (2013) Simulation of active skeletal muscle tissue with a transversely isotropic viscohyperelastic continuum material model. *Proceedings of the Institution of Mechanical Engineers, Part H: Journal of Engineering in Medicine*, **227**(5): pp. 571-580

[9] Begeman, P., King, A., Levine, R., and Viano, D.C. (1980) Biodynamic response of the musculoskeletal system to impact acceleration, SAE Technical Paper.

[10] Brolin, K., Hedenstierna, S., Halldin, P., Bass, C., and Alem, N. (2008) The importance of muscle tension on the outcome of impacts with a major vertical component. *International Journal of Crashworthiness*, **13**(5): pp. 487-498.

[11] Brolin, K., Halldin, P., and Leijonhufvud, I. (2005) The effect of muscle activation on neck response. *Traffic injury prevention*, **6**(1): pp. 67-76.

[12] Meijer, R., Van Hassel, E., *et al*. Development of a multi-body human model that predicts active and passive human behaviour. *Proceedings of the International Conference on Biomechanics of Impact IRCOBI, Dublin-Ireland*, 2012.

[13] Östh, J., Brolin, K., and Happee, R. (2012) Active muscle response using feedback control of a finite element human arm model. *Computer methods in biomechanics and biomedical engineering*, **15**(4): pp. 347-361.

[14] Kistemaker, D.A., Van Soest, A.K.J., and Bobbert, M.F. (2006) Is equilibrium point control feasible for fast goal-directed single-joint movements? *Journal of Neurophysiology*, **95**(5): pp. 2898-2912.
[15] Oliveira, A.R., Gonçalves, S.B., de Carvalho, M., and Silva, M.T. (2016) Development of a musculotendon model within the framework of multibody systems dynamics. *Computational Methods in Applied Sciences*, **42**: pp. 213-237.
[16] Ambrósio, J.A. and Kecskeméthy, A. Multibody dynamics of biomechanical models for human motion via optimization. *Multibody Dynamics*. pp. 245-272. *Springer*, 2007
[17] User Manual: M50 Occupant Version 4.3 for LS-DYNA.
[18] Gayzik, F.S., Moreno, D.P., Vavalle, N.A., Rhyne, A.C., and Stitzel, J.D. Development of the Global Human Body Models Consortium mid-sized male full body model. *Proceedings of the Injury Biomechanics Research Thirty-Ninth International Workshop*, 2011.
[19] Cronin, D.S. (2014) Finite element modeling of potential cervical spine pain sources in neutral position low speed rear impact. *Journal of the mechanical behavior of biomedical materials*, **33**: pp. 55-66.
[20] Fice, J.B. and Cronin, D.S. (2012) Investigation of whiplash injuries in the upper cervical spine using a detailed neck model. *Journal of biomechanics*,. **45**(6): pp. 1098-1102.
[21] Panzer, M.B. and Cronin, D.S. (2009) C4–C5 segment finite element model development, validation, and load-sharing investigation. *Journal of biomechanics*, **42**(4): pp. 480-490.
[22] Panzer, M.B., Fice, J.B., and Cronin, D.S. (2011) Cervical spine response in frontal crash. *Medical engineering & physics*, **33**(9): pp. 1147-1159.
[23] Ivancic, P., Panjabi, M.M., Ito, S., Cripton, P., and Wang, J. (2005) Biofidelic whole cervical spine model with muscle force replication for whiplash simulation. *European spine journal*, **14**(4): pp. 346-355.
[24] Panjabi, M.M., Ito, S., Pearson, A.M., and Ivancic, P.C. (2004) Injury mechanisms of the cervical intervertebral disc during simulated whiplash. *Spine*, **29**(11): pp. 1217-1225.
[25] Panjabi, M.M., Pearson, A.M., *et al*. Cervical spine ligament injury during simulated frontal impact. *Spine*, 2004. **29**(21): pp. 2395-2403.
[26] Pearson, A.M., Ivancic, P.C., Ito, S., and Panjabi, M.M. (2004) Facet joint kinematics and injury mechanisms during simulated whiplash. *Spine*, **29**(4): pp. 390-397.
[27] Ito, S., Ivancic, P.C., *et al*. (2005) Cervical intervertebral disc injury during simulated frontal impact. *European Spine Journal*, **14**(4): pp. 356-365.
[28] Davidsson, J., Deutscher, C., Hell, W., Lövsund, P., and Svensson, M.Y. (2001) Human volunteer kinematics in rear-end sled collisions. *Crash prevention and injury control*, **2**(4): pp. 319-333.
[29] Hynd, D., Svensson, M., Trosseille, X., van Ratingen, M., and Davidsson, J. (2007) Dummy requirements and injury criteria for a low-speed rear impact whiplash dummy. *European Enhanced Vehicle-Safety Committee, EEVC WG12 A*, **505**: pp. 2007.
[30] Thunnissen, J., Wismans, J., Ewing, C., and Thomas, D. Human volunteer head-neck response in frontal flexion: a new analysis. *Proceedings of Stapp Car Crash Conference*, 1995.
[31] Wismans, J., Van Oorschot, H., and Woltring, H. (1986) Omni-directional human head-neck response. SAE Technical Paper.
[32] Winters, J.M. (1995) An improved muscle-reflex actuator for use in large-scale neuromusculoskeletal models. *Annals of biomedical engineering*, **23**(4): pp. 359-374.
[33] Zajac, F.E. (1988) Muscle and tendon: properties, models, scaling, and application to biomechanics and motor control. *Critical reviews in biomedical engineering*, **17**(4): pp. 359-411.
[34] Winters, J.M. and Woo, S.L. (1990) *Multiple muscle systems: Biomechanics and Movement Organization*.
[35] Ito, Y., Corna, S., von Brevern, M., Bronstein, A., and Gresty, M. (1997) The functional effectiveness of neck muscle reflexes for head-righting in response to sudden fall. *Experimental brain research*, **117**(2): pp. 266-272.
[36] Iwamoto, M., Nakahira, Y., and Kimpara, H. (2015) Development and validation of the Total HUman Model for Safety (THUMS) toward further understanding of occupant injury mechanisms in precrash and during crash. *Traffic injury prevention*, **16**(sup1): pp. S36-S48.
[37] Günther, M., Schmitt, S., and Wank, V. (2007) High-frequency oscillations as a consequence of neglected serial damping in Hill-type muscle models. *Biological Cybernetics*, **97**(1): pp. 63-79.
[38] Garrett, W.E., Safran, M.R., Seaber, A.V., Glisson, R.R., and Ribbeck, B.M. (1987) Biomechanical comparison of stimulated and nonstimulated skeletal muscle pulled to failure. *The American journal of sports medicine*, **15**(5): pp. 448-454.

[39] Lieber, R.L. and Friden, J. (1993) Muscle damage is not a function of muscle force but active muscle strain. *Journal of Applied Physiology*, **74**(2): pp. 520-526.

[40] Gehre, C., Gades, H., and Wernicke, P. Objective rating of signals using test and simulation responses. *Proceedings of 21st International Technical Conference on the Enhanced Safety of Vehicles Conference (ESV),* 2009.

[41] Brault, J.R., Siegmund, G.P., and Wheeler, J.B. (2000) Cervical muscle response during whiplash: evidence of a lengthening muscle contraction. *Clinical biomechanics*, **15**(6): pp. 426-435.

[42] Beeman, S.M., Kemper, A.R., Madigan, M.L., Franck, C.T., and Loftus, S.C. (2012) Occupant kinematics in low-speed frontal sled tests: Human volunteers, Hybrid III ATD, and PMHS. *Accident Analysis & Prevention*, **47**: pp. 128-139.

[43] Kamibayashi, L.K. and Richmond, F.J. (1998) Morphometry of human neck muscles. *Spine*, **23**(12): pp. 1314-1323.

[44] Hatze, H. (1978) A general myocybernetic control model of skeletal muscle. *Biological cybernetics*, **28**(3): pp. 143-157.